Wind dependence of ambient noise in a biologically rich coastal area

Delphine Mathias, Cédric Gervaise, Lucia Di Iorio

Wind dependence of ambient noise in a biologically rich coastal area

Delphine Mathias
Socété d'Observation Multi-Modale de l'Environnement, 115 Rue Claude Chappe, 29280 Plouzané, France

Cédric Gervaise and Lucia Di Iorio
Chaire Chorus, Foundation of the Grenoble Institute of Technology, 46 Rue Felix Viallet, 38031 Grenoble, France

Electronic mail: delphine.mathias@gmail.com

Abstract

The wind dependence of acoustic spectrum between 100 Hz and 16 kHz is investigated for coastal biologically rich areas. The analysis of 5 months of continuous measurements run in a 10 m deep shallow water environment off Brittany (France) showed that wind dependence of spectral levels is subject to masking by biological sounds. When dealing with raw data, the wind dependence of spectral levels was not significant for frequencies where biological sounds were present (2 to 10 kHz). An algorithm developed by Kinda, Simard, Gervaise, Mars, and Fortier [J. Acoust. Soc. Am. 134(1), 77–87 (2013)] was used to automatically filter out the loud distinctive biological contribution and estimated the ambient noise spectrum. The wind dependence of ambient noise spectrum was always significant after application of this filter. A mixture model for ambient noise spectrum which accounts for the richness of the soundscape is proposed. This model revealed that wind dependence holds once the wind speed was strong enough to produce sounds higher in amplitude than the biological chorus (9 kn at 3 kHz, 11 kn at 8 kHz). For these higher wind speeds, a logarithmic affine law was adequate and its estimated parameters were compatible with previous studies (average slope 27.1 dB per decade of wind speed increase).

I. INTRODUCTION

A. Marine soundscapes

The ocean acoustic environment, called the "marine soundscape," consists of biological (biophony), abiotic (geophony) and anthropogenic (man-made) sounds (Pijanowski et al., 2011). These marine soundscapes are integrative fingerprints of ecosystems, thus allowing remote sensing of various sound sources. Biological sound sources include marine mammals (Mellinger et al., 2007), fishes (Rountree et al., 2006), and benthic organisms (Watanabe et al., 2002; Radford et al., 2008; Di Iorio et al., 2012). Abiotic sound sources include physical processes such as underwater seismic and volcanic events (Vandemeulebrouck et al., 2000), ice dynamics (Kinda et al., 2013), and meteorological events (Riser et al., 2008; Nystuen et al., 2010). Contributors to anthropogenic noise are classically commercial shipping (McDonald et al., 2008; Gervaise et al., 2012), offshore and shallow water resources exploration, marine constructions, marine renewable energies, and recreational activities (Hildebrand, 2009).

Identifying and describing the features of different soundscape contributors allows to understand and monitor the environmental status of marine environments (National Research Council, 2003). Soundscapes are always the sum of close identifiable sources and a chorus of a myriad of distant sources producing what is typically called the ambient noise (Urick, 1984; Wenz, 1962). These soundscapes are therefore rich in information on biological, geological, climatic, and human activities. Monitoring the sound field is an effective mean to gauge and track biological activity, species presence and diversity, and evaluate the ecosystem health.

B. Meteorological forcing in marine ecosystems

Monitoring meteorological parameters and their variations is of critical ecological relevance, e.g., in Polar Regions for the assessment of the effects of global warming (Post et al., 2009; Schofield et al., 2010). Meteorological forcing also plays a major role in the ocean's physical circulation and primary production, as it is coupled to the dynamics of the mixed layer (Falkowski et al., 1998). For instance, wind-induced phenomena increase the flux of nutrients from deeper, nutrient-rich waters to the mixed layer and are thus responsible for driving phytoplankton production (Walsh et al., 1978). Wind-driven circulations also have a major influence on larval dispersal and transport (Lee et al., 1992). Despite their importance, meteorological conditions are difficult to measure in situ using long-term surface anemometers and rain gauges (Vagle et al., 1990).

C. Monitoring of wind speed at sea with passive acoustics

Recent development in fixed autonomous recorders (Sousa-Lima et al., 2013) and ocean observatories (such as

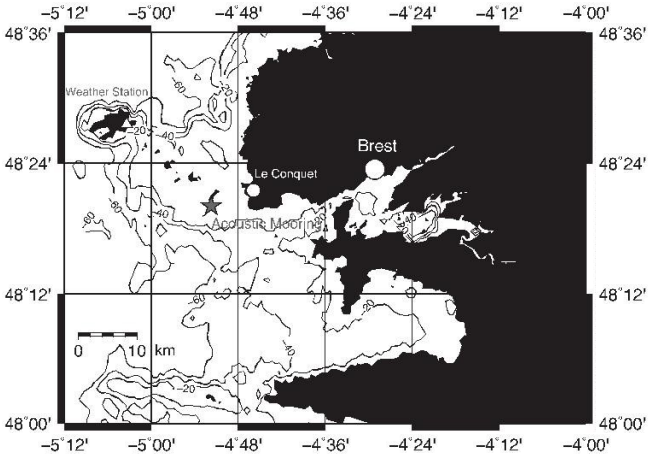

FIG. 1. Contour map (depth in meters) of the study area. The location of the acoustic mooring is 48.33◦N, 4.86◦W on the continental shelf in water about 10 m deep (±3 m depending on the tide) in the Iroise Natural Marine Park.

the ALOHA, NEPTUNE, and LIDO observatories) allows for long-term acoustic measurements across all oceans and passive acoustics has become an efficient method for monitoring rain and wind speed. Early work by Knudsen (1948) and Wenz (1962) showed that in deep waters, sea surface agitation (rain, wind) is the dominant factor of ambient noise levels above 1 kHz. These two components of the geophony are generated on one hand by rain drops generating broadband impact noise and dragging air into the surface layer, forming bubbles (Nystuen *et al.*, 1993; Prosperetti et Oguz, 1993) and on the other hand by breaking waves from wind-generated whitecaps that create a cloud of bubbles radiating sound via individual and collective oscillations (Medwin and Beaky, 1989). Several authors described the depth dependence of ambient noise in the deep ocean environment (Perrone, 1970; Morris, 1978; Marshall, 2005; Gaul *et al.*, 2007; Barclay and Buckingham, 2013) and derived empirical relationships linking wind speed to ambient noise level (Wenz, 1962; Evans *et al.*, 1984; Lemon *et al.*, 1984; Vagle *et al.*, 1990; Vakkayil *et al.*, 1996; Zedel *et al.*, 1999). Vagle *et al.* (1990) derived an empirical algorithm linking linearly the sound pressure level at 8 kHz with wind speed (at a 10 m height), using acoustic instruments deployed below 93 m depth. Estimated wind speeds were within 0.5 m/s of anemometer measurements for wind speeds between 4 and 15 m/s. Vagle *et al.* (1990) mentioned that the relationship does not hold in shallow waters because of environmental factors such as industrial noise, bottom effects, or wind fetch. Indeed in shallow coastal waters, anthropogenic noise sources and biological sounds have a greater influence on the soundscape than in deep waters. Previous shallow water studies showed that ambient noise varies greatly with location and season, due to sound speed, bottom properties, and wind speed variations (Piggot, 1964; Ingenito and Wolf, 1989; Weston and Ching, 1989; Wille and Geyer, 1984; Hazen and Desharnais, 1997; Ramji *et al.*, 2008). Piggot (1964), Lemon *et al.* (1984), Zakarauskas *et al.* (1990), and Ramji *et al.* (2008) reported that ambient noise levels for a given wind speed are up to 10 dB higher than those measured in deep water. Most shallow water studies mention that data corrupted by traffic noise and/or marine mammal sounds were excluded from the analysis when studying the wind dependence of ambient noise (McDonald *et al.*, 2008; Poikonen and Madekivi, 2010). To our knowledge, no peer-reviewed publication addressed the wind dependence of shallow water ambient noise in the presence of numerous biological transient sounds from benthic origin [e.g., snapping shrimps (*Decapoda, Alpheidae*)].

D. Paper's objectives

In this study, we report on the dependency of shallow water ambient noise level on wind speed in the Iroise Sea, a biologically rich coastal area off Brittany, France. Transient zoobenthic sounds were consistently present and contributed most to the overall received sound pressure level. Although present only 4.8% of the time, these individually identifiable biotic sounds represented 82% of the acoustic energy (see Fig. 2). These zoobenthic sounds masks the underlying ambient noise and does not allow a direct assessment of environmental ambient noise drivers such as wind speed. The soundscape of the Iroise Sea with its biophonic predominance is therefore a good representative of soundscapes of temperate or tropical coastal environments.

The objective of this paper is to explore the wind dependence of the spectral level of two different acoustic descriptors of the soundscape for frequencies ranging from 100 to 16 000 Hz. The first descriptor is the power spectral density level of the raw acoustic data (γRL dB re. 1 μPa^2/Hz) in the presence of biotic transient sounds (here referred to as "overall ocean noise level"), whereas the second descriptor is the estimated power spectral density level of the underlying background ambient noise (γANL dB re. 1μPa^2/Hz) when biotic transient sounds have been removed from the data (here referred to as "ambient noise level"). Section II describes the study area and data collection, including acoustic recordings and wind speed measurements. Section III explains the methodology for extracting the ambient noise in the presence of transient impulsive sounds, previously applied for the analysis of arctic soundscape by Kinda *et al.* (2013). Section IV shows the dependence of the overall ocean noise spectrum and ambient noise spectrum to wind speed at several frequencies of interest and presents how the dependence of ambient noise on wind speed can be parameterized with a logarithmic model. In Sec. V, results are discussed and compared to reference work by Wenz (1962) and previous shallow water studies.

II. DATA COLLECTION

A. Study site

The study site is located in the Mole`ne Archipelago (48◦20.069' N; 4◦51.701' W), which is part of the Iroise Natural Marine Park, a marine protected area located in Western Brittany, France. The archipelago is a shallow water area that comprises 11 islands. The area hosts a rich biodiversity and biomass with the largest seaweed fields in Europe, a wide range of zoobenthic species (e.g., over 300 crustacean, 200 mollusk species), endangered birds and marine mammals, including bottlenose dolphins (*Tursiops*

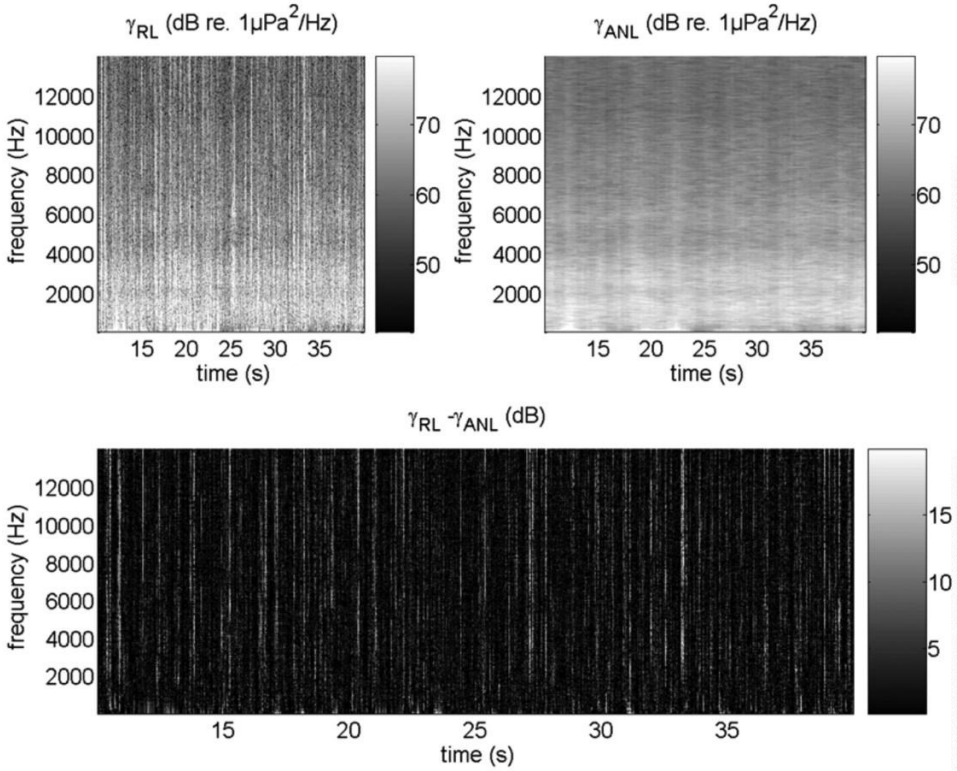

FIG. 2. Spectrogram (Hanning window, L = 1024, 50% overlap) of a typical 40 s long segment of overall ocean noise (top-left panel) showing a myriad of individual transient signals, and of the estimated background ambient noise (top-right panel) obtained with $Q = 0.2$ lacking individually identifiable transient signals. The difference between the overall ocean noise spectrum γ^{RL} (f) and the background ambient noise spectrum γ_{ANL} (f) is shown in the bottom panel. Loud short benthic impulses have been filtered out using the Kinda filtering process. For this snapshot, the raw data root-mean-squared sound pressure level (SPL) over 1.5 to 16 kHz is 112 dB re. 1 μPa,^{2} the mean ambient noise level is 100.5 dB re. 1 $^{\mu}$Pa,^{2} the proportion of impulsive sounds whose level is higher than ambient noise level by 9 dB is 0.065. When exploring the whole data set, the raw data root-mean-squared SPL over 1.5 to 16 kHz averages 109.25 $\pm$ 0.81 dB re. 1 μPa,^{2} the mean ambient noise level averages 101.52 $^{\pm}$ 1.65 dB re. 1 $^{\mu}$Pa,^{2} and finally the proportion of impulsive sounds whose level is higher than ambient noise level plus 9 dB averages 0.048 $\pm$ 0.13.

truncatus) and grey seals (*Halichoerus grypus*) (Raffin, 2004). Anthropogenic activities in the area mainly include small local commercial fishing and yachting (Talidec *et al.*, 2002). The small harbor of Le Conquet (2500 inhabitants) is located 7 km from the recording site, whereas the busy harbor of Brest (221 600 inhabitants) is about 20 km away (Fig. 1).

B. Acoustic recordings and wind speed data

An AURAL-M2 autonomous underwater recorder (Multi-Electronique, Rimouski, QC) was moored south of Beniguet island, 70 cm above the bottom in water about 10 m deep ($\pm$3 m depending on the tide) from June 20, 2011 to November 13, 2011 (Fig. 1). The mooring was deployed on the ocean floor by a boat and divers fixed the autonomous recorder onto the mooring. This technique does not require a mooring line and therefore strongly limits cable-strumming noise. Any residual hydrodynamic noise is well below the ambient noise level. Bottom properties of the deployment location correspond to infralittoral coarse sediments. The AURAL was programmed to record continuously with a 32 768 Hz sampling frequency and 16 bits resolution. The AURAL used a wideband omnidirectional calibrated HTI-96 min hydrophone (High-Tech Inc.) with a flat frequency response over the 10 Hz to 24 kHz range and sensitivity of $_$163 dB re. 1 μPa/V. The AURAL recorder was calibrated before the *in situ* recording session by acquiring four 10-min sessions in Brest harbor with a fully calibrated (but non autonomous) Bruel & Kjaer measurement chain (Hydrophone B&K 8106 and Nexus Signal conditioner). The spectra from the two devices were estimated and equalized to deduce the sensibility of the AURAL HTI 96 min hydrophone over a 10 Hz to 30 kHz bandwidth.

Hourly mean wind speed data (at a standard 10 m height) at the study site were obtained from Previmer (2016) model outputs (ARPEGE model). The model uses a 50 km grid size. These wind speeds values were similar (within 0.5 kn) to wind speeds (at a standard 10 m height) measured at the Ouessant-Stiff weather station, situated on an island located 12 km north of the acoustic recording deployment.

III. METHODS

A. Estimation of "overall ocean noise" and "background ambient noise" spectrum levels

Acoustic data processing was conducted following the same method than the one used by Kinda *et al.* (2013) in an Arctic study. Acoustic recordings were cut into 10-s bins. For each bin, one estimate of the overall ocean noise spectrum levels [γRL(f); dB re. 1 μPa^2/Hz] and one estimate of the background ambient noise spectrum levels [γANL (f); dB re. 1 μPa^2/Hz] were computed. The raw acoustic measurement (calibrated, unfiltered) used to compute γRL(f) was assumed to be the sum of the stationary, Gaussian

background ambient noise, and the short transient sounds from benthic animals (Fig. 2, top-left box). The measurements were fast Fourier transformed (Hanning window, 1024-point FFT, 50% overlap), yielding a 32 Hz frequency resolution. Each 10-s bin produced 640 estimates of the power spectrum levels. The overall ocean noise spectrum γ RL(f) was obtained by averaging these 640 spectrum levels prior to their conversion into decibels. To estimate the background ambient noise spectrum γANL(f) at a given frequency f_0, the collection of the 640 samples was sorted in ascending order. With Q being a low percentile (from 0.04 to 0.2) of the ranked power spectral density levels and $g_Q(f_0)$ the value of this percentile at frequency f_0, then the value of the ambient noise spectrum level was estimated with Eq. (1)

$$\gamma_{\mathrm{ANL}}(f_0) = -\frac{\gamma^Q(f^0)}{\log(1-Q)}. \tag{1}$$

This equation exploits the fact that if the ambient noise is normally distributed, then its power spectral density level follows a centered chi-squared distribution with two degrees of freedom (Kay, 1998). Furthermore, for samples of background ambient noise alone, spectrum levels are likely to correspond to the smaller values of the analysis bins, and if the percentile Q is small enough, $g_Q(f_0)$ is relative to the background ambient noise only, thus filtering out the loud biotic transient sounds. The algorithm to compute γ ANL(f) is fully detailed in Kinda *et al.* (2013). Figure 2 illustrates its efficiency on a 40-s snapshot, with Q equal to 0.2. As the temporal dynamic of wind is much more than 10 s, wind-induced sound is stationary at this scale, so that wind contribution is not filtered out during the estimation stage of γ ANL(f) whereas the loud short impulses are rejected.

The narrowband γ RL and γ ANL values at 400 Hz, 3 kHz, and 8 kHz were computed in each 10-s bin; 400 Hz belongs to the frequency band free of benthic sounds and is appropriate to look at the low frequency relationship between ambient noise and wind speed; 3 kHz is the peak frequency of benthic transient sounds (cf. Sec. IV A); and 8 kHz is commonly used in the literature to study relationship between wind, rain, and ambient noise level (Vagle *et al.*, 1990; Zedel *et al.*, 1999; Ma *et al.*, 2005; Nyusten *et al.*, 2010).

Time series of γ RL and γ ANL covering the 5-month dataset were obtained by computing the median value in successive 20-min segments. Basic statistics were then computed from the distribution of these 5-month time series and Pearson correlation coefficients between each acoustic spectral quantity (γ RL and γ ANL) and the logarithm of the wind speed were evaluated. Several length of averaging windows were examined, and it was found that 20-min was the length generating the highest correlation between spectral quantities (γ RL and γ ANL) and wind speed events. Figure 6 shows that there is no time lag between a high wind speed event and an increase in ambient noise level.

B. Logarithmic model for wind speed dependence of noise spectrum levels and parameterization

The wind speed time series was binned into overlapping 1 kn bins. Narrowband γ RL 203 and γ ANL at 400 Hz, 3 kHz, and 8 kHz were plotted as a function of wind speed. The characteristics of noise level dependence on wind speed were parameterized using a multi-parameter logarithmic model. The model was constituted of two parts, a constant floor corresponding to the biological and the anthropogenic contributions (Q_f, dB re. 1μPa^2/Hz) and the wind speed contribution (Q_w, dB re. 1μPa^2/Hz) to the ambient noise. Logarithmic expressions have been frequently used to model ambient noise levels as a function of wind speed (Vagle *et al.*, 1990; Zedel *et al.*, 1999; Ma *et al.*, 2005; Nyusten *et al.*, 2010). The following mathematical expressions were used to model γRL and γ ANL as a function of wind speed W (in knots):

$$\gamma^m(Q^f, Q^1, k, W) = 10\log^{10}(10^{Q_f/10} + 10^{Q_w/10}), \tag{2}$$

with

$$Q^w = Q^1 + k\log^{10}(W), \tag{3}$$

where g_m corresponds to either γ RL and γ ANL in dB re. 1 μPa^2/Hz at a given frequency f_0. The overall ocean noise and background ambient noise levels were modeled as the sum of two components, the wind-induced sound and all the other sonic contributions. We assume these two components to be independent so that their power spectral densities can be summed in the linear scale. The power spectral density of the wind contribution [Eq. (3)] is a log-affine law where Q_1 is the power spectral density for wind speeds equal to 1 kn and k is the rate of the law expressed in dB per decade. The complementary contribution is assumed to be a floor level (Q_f dB re. 1μPa^2/Hz) that does not depend on wind speed. This three-parameters (Q_f, Q_1, k) model for wind dependence of spectral levels account for potential masking of wind noise by other sonic contributions. Therefore, a fourth parameter is introduced, the wind speed of transition (W_t) representing the wind speed threshold at which the wind component starts to exceed the floor level ($Q_w \geq Q_f$). W_t is given by

$$W_t = 10^{(Q^f - Q^1)/k}. \tag{4}$$

Using the triplet of parameters (Q_f, W_t, k), the wind dependence model of the power spectral density g at frequency f_0 becomes

$$\gamma = Q_f + 10\log_{10}\left[1 + \left(\frac{W}{W_t}\right)^{k/10}\right]. \tag{5}$$

This log-affine model is coherent with the ones used in previous studies (Ramji *et al.*, 2008; Poikonen and Madeviki, 2010; Nystuen *et al.*, 2010). Figure 3 illustrates the proposed wind dependence model of the power spectral density (with $Q^f = 60$ dB re. 1μPa^2/Hz, $Q^1 = 25$ dB re.1Pa^2/Hz, $W^t = 10$ kn, $k = 27$ dB/dec).

Estimations of the triplet of parameters $\{Q_f, Q_1, k\}$ were performed for γ RL and γ ANL at frequencies f_0 equal to 400 Hz, 3 kHz, and 8 kHz. For each frequency and acoustic spectral quantity (γ RL and γ ANL), a bootstrap method was used to estimate the best triplet of parameters and to assess their accuracy. For one iteration of the bootstrap, a set of one

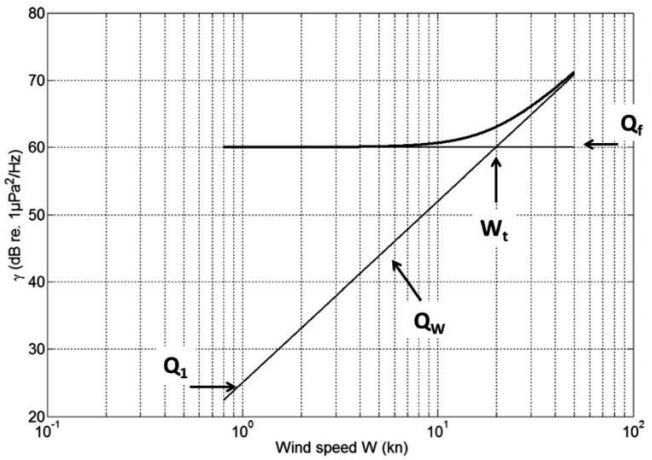

FIG. 3. Illustration of the model: the power spectral density is the sum of a constant-floor power spectral level Q_f (dB re. 1 μPa^2/Hz) and a log-affine law Q_w with intercept equal to Q_1 (dB re. 1 μPa^2/Hz) and rate equal to k (dB/decade). The log-affine law and floor level intercept at a transition wind speed W_t. At this wind speed, $\gamma = Q_f + 3$ dB.

thousand 20-min segments were randomly chosen among the available 10 800 segments. A least-mean-square method was used to find the best fit (optimal triplet $\{Q_f, Q_1, k\}$) between the model and the measured γ RL and γ ANL values. One hundred bootstrap iterations were conducted using the simplex search algorithm of Lagarias *et al.* (1998). The final estimate of $\{Q_f, Q_1, k\}$ was the average over the 100 iterations, with the accuracy of the estimation represented by the standard deviation of each parameter.

IV. RESULTS

A. Characteristics of overall ocean noise and background ambient noise levels

Figure 4 displays a 4-day long-term spectral average of ocean noise and illustrates the main components of the recorded soundscape. The frequency range can be divided into three frequency bands. The band from 0 to 1.5 kHz presents a distinctive daily pattern with a higher level during daytime than during nighttime (average difference ~8 dB). This diel variability is likely due to the anthropogenic contributions from the harbors of Brest and Le Conquet (unpublished data). The band from 1.5 to 6 kHz is dominated by benthic sounds (both distant choruses and close transient impulses). Previous work identified snapping shrimps and sea urchins as potential sources of benthic noise in this area (Raffin, 2004; Di Iorio *et al.*, 2012) with a maximum power spectral density located around 3 kHz. Although this band is representative for the benthic production of sounds, anthropogenic and benthic sounds may overlap at the lower part of it. The band from 6 to 16 kHz contains only benthic sounds with the same diel variation as in the 1.5 to 6 kHz band (unpublished data).

Figure 5 displays the overall ocean noise [γ RL(f), left panel] and background ambient noise spectrum levels [γ ANL(f), right panel] for various wind speeds, ranging from 2 to 22 kn. Superimposed upon these results are the wind-alone Wenz curves for wind speeds ranging from 2 to 25 kn. γ RL(f) and γ ANL(f) share a set of features. Both spectra are flat for frequencies smaller than 2 kHz with levels falling within the range of the Wenz curves. There is a spectrum level increase between 2 and 5 kHz with a spectral peak at 3 kHz. The rich benthic activity explains why levels are about 8 dB higher than those reported by Wenz (1962) for similar wind speed conditions above 1 kHz. Above 3 kHz, there is a spectral decline with a slope of -17 dB/decade (-5.1 dB/octave). This slope is similar to Wenz' spectral slope above 1 kHz.

A comparison of the γ RL(f) and γ ANL(f) spectra reveals that overall ocean noise levels exceed background ambient noise levels by 4 dB for frequencies below 2 kHz. This difference increases up to 7 dB at 3 kHz and remains

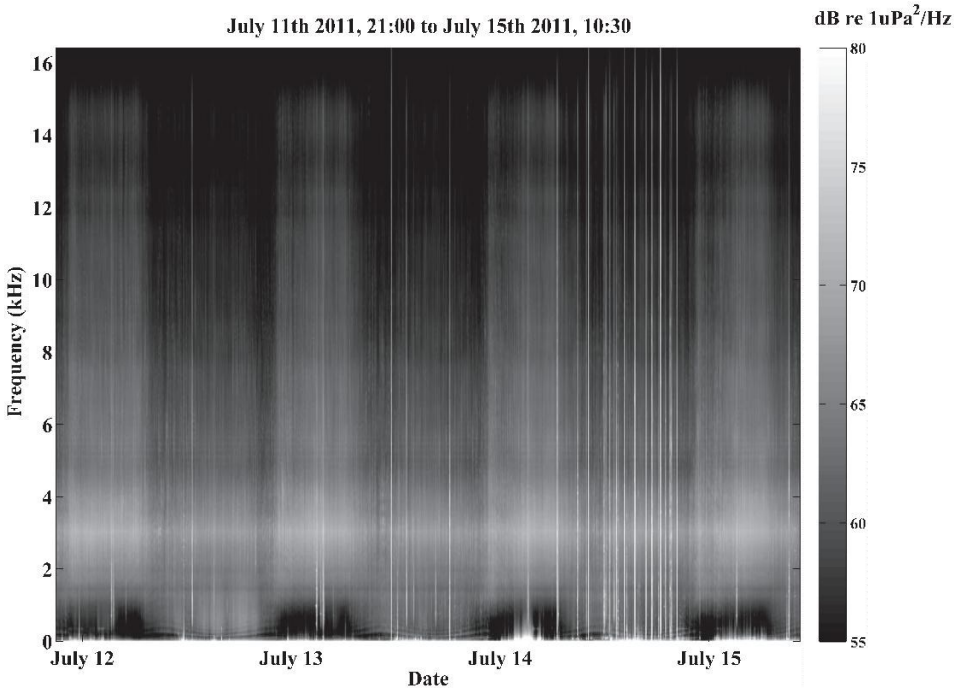

FIG. 4. The 4-day long-term spectral average of overall ocean noise, units are dB re 1 μPa^2/Hz. The band from 0 to 1.5 kHz presents a distinctive daily pattern with a higher level during daytime than during nighttime due to shipping activity (average difference ~8 dB). The band from 1.5 to 6 kHz is dominated by benthic sounds (both distant choruses and close transient impulses). Wideband vertical stripes are distinctive of boats that came close to the recorder. One can also notice the high number of transient sounds on July 14 (French national day), corresponding to an high occurrence of recreational boats in the study area.

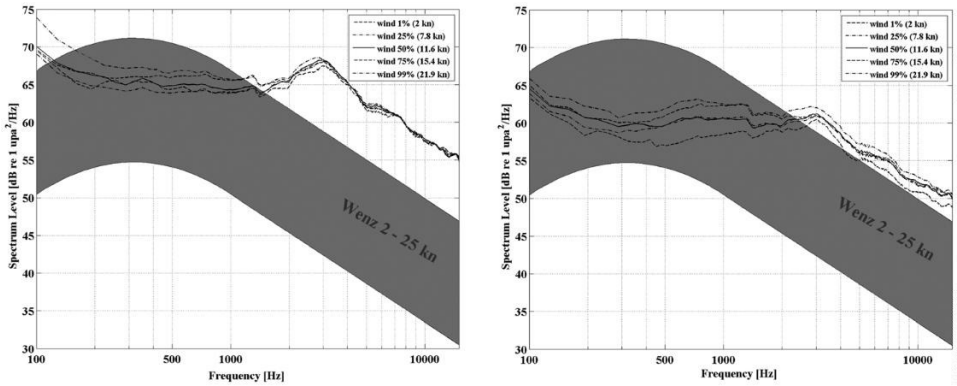

FIG. 5. Overall ocean noise spectrum level $\gamma_{RL}(f)$ (left panel) and ambient noise spectrum level $\gamma_{ANL}(f)$ (right panel) for wind speeds corresponding to the 1st, 25th, 50th, 75th and 99th percentile. The Wenz curves (shaded grey areas) for the same extent of wind speed conditions are shown for comparison.

constant up to 14 kHz. γ RL(f) and γ ANL(f) both positively depend on wind speed for frequencies below 1 kHz. Above 1 kHz and up to 14 kHz, the wind-dependence only persists for γ ANL(f), while it disappears for γ RL(f). This suggests that the benthic sounds mask the wind-induced noise.

B. Wind speed and noise level times series

For the period from June 20 to November 13, 2011, wind speeds ranged from 2 to 25.5 kn with a mean value of 12 kn. Table I reports the wind speed percentile distribution during the measurement period.

Table II displays the distribution statistics of ocean noise levels (γ RL) and ambient noise levels (γANL) at 400 Hz, 3 kHz, and 8 kHz. Figure 6 illustrates the dependence between γ RL or γ ANL and wind speed. It shows the 3 kHz γ RL and γ ANL time series over a 1-month period along with the corresponding wind speed times series. The γ RL at 3 kHz is modulated by the diel benthic sound fluctuations. These fluctuations are less important but still present on the γANL time series since the transient contributions have been removed and only the background chorus remains. High wind speed events are closely correlated with increases in γANL (cf. arrows on Fig. 6). In contrast, high wind speed events are not associated with significant γRL increases as indicated by the Pearson correlations computed between the logarithm of the wind speed and γRL or γANL at 400 Hz, 3 kHz, and 8 kHz (Table III). The diurnal variation is more important during periods of low wind conditions, and can reach as much as 9 dB.

Correlation between γ ANL and the wind speed logarithm decreases with frequency ($r = 0.68$ at $f = 400$ Hz, $r = 0.46$ at $f = 3$ kHz, $r = 0.31$ at $f = 8$ KHz). γ RL and the logarithm of wind speed are positively correlated for $f = 400$ Hz ($r = 0.52$). This correlation decreases dramatically at 3 and 8 kHz ($r = 0.16$, $r = 0.06$).

C. Noise level and wind speed logarithmic model

Figure 7 displays the wind dependence of γ RL and γ ANL at 400 Hz, 3 kHz, and 8 kHz. Black lines indicate the

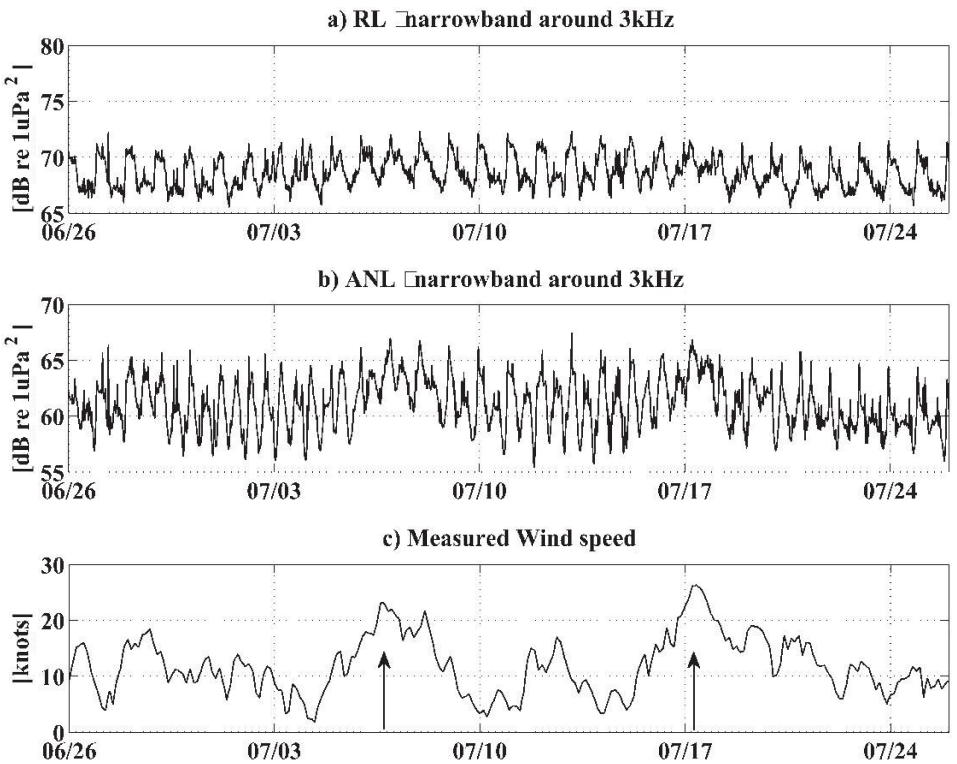

FIG. 6. Time series of (a) overall ocean noise level (γ_{RL}) and (b) background ambient noise level (γ_{ANL}) at 3 kHz during the period from June 26 to July 26 2011. (c) The corresponding wind speed time series. Arrows indicate wind speed peaks.

TABLE I. Wind speed distribution during the experiment (June 21, 2011 to November 13, 2011).

	Mean	Std	1%	5%	10%	25%	50%	75%	90%	95%	99%
Wind speed (kn)	12.0	5.6	2.0	4.0	5.2	7.8	11.6	15.4	19.5	21.9	25.5

best fit between the logarithmic model and the noise measurements. Table IV summarizes the best-fit parameters.

Estimations of the three parameters of the wind components $\{Q_1, k, W_t\}$ are accurate for γ RL at 3 kHz but the wind dependence is not significant (F-test = 210, $p > 0.05$). The inaccurate estimations of $\{Q^1, k, W^t\}$ at 8 kHz lead to a non-significant wind dependence (F-test = 154, $p > 0.05$). At 3 and 8 kHz, although there is a small increase of γ RL for wind speeds higher than 15 kn, there is not a clear relationship between γ RL and wind speed, suggesting that the wind-induced noise is totally masked by biotic sounds. This corroborates the large values of wind speed transition obtained at these frequencies ($W^t = 15.5 \pm 3.5$ kn at 3 kHz and $W^t = 16.1 \pm 4.1$ kn at 8 kHz).

In contrast, at 400 Hz for both γ RL and γ ANL and at 3 kHz and 8 kHz for γ ANL, the estimation of our model parameters are accurate, implying a good fit of the model, and show a significant wind dependence (F equal to 680, 773, 457, and 344, respectively; $p < 0.05$). These four cases present similar k values (29 ± 4 dB/decade). The four cases differ with respect to the transition wind speed, which increases with frequency (3.3 ± 0.2 kn at 400 Hz; 9.9 ± 0.3 kn at 3 kHz; 11.8 kn $\pm$ 0.9 kn at 8 kHz) thus suggesting an increasing masking of biophonic chorus with frequency.

V. DISCUSSION

A. Wind dependence of ambient noise level acoustic descriptor and masking by biological sounds

The results of this study clearly show that in coastal biologically rich areas, the acoustic wind dependence can be assessed, but only after removal of zoobenthic transient sounds (e.g., snapping shrimp). Soundscapes in such habitats are in fact principally composed of an elevated number of identifiable transient sounds emitted by close benthic fauna and an underlying stationary chorus (i.e., background ambient noise). Spectrum levels of the overall ocean noise (γ RL), which include transient benthic signals are 5.4 dB higher at 400 Hz, 7 dB higher at 3 kHz, and 6 dB higher at 8 kHz than those of background ambient noise alone (γ ANL). This difference is caused by broadband transient benthic sounds whose peak frequency is around 3 kHz.

The masking of wind dependence by the presence of benthic sounds is also emphasized when comparing power spectrum levels of the overall ocean noise and the background ambient noise only with those reported by Wenz (1962). In fact, γ ANL follows the Wenz curves, whereas γ RL exceeds the maximal value of the Wenz spectra by 10 dB for frequency above 1 kHz reaching a maximum at 3 kHz. This increase in spectral energy corresponds to the presence of transient benthic signals that mask the wind dependence of γ RL. Below 1 kHz, both γ RL and γ ANL are relatively constant within the range of the Wenz curves. At these low frequencies, both noise levels are sensitive to wind speed and anthropogenic contributions. To significantly influence sound levels, sonic wind contribution has to exceed the biotic contribution. Although largely explained by the wind component, background ambient noise levels are also affected by the chorus of distant sounds of benthic origin. This is revealed by the small peak at 3 kHz in the background ambient noise spectra which corresponds to the spectral peak of benthic animals (e.g., snapping shrimps) recorded in the area (Fig. 5).

At 400 Hz, both overall ocean noise level (γ RL) and background ambient noise level (γ ANL) are a linear function of wind speed. At 3 and 8 kHz, although there is a small increase of γ RL for winds higher than 15 kn, there is not a clear relationship between γ RL and wind speed. This is explained by the domination of benthic organism sounds at those frequencies. In contrast, there is a significant positive relationship between wind speed and γ ANL at 3 and 8 kHz. This is explained by the absence of transient sounds produced by benthic organisms thus limiting the masking effect on the background ambient noise level. However, the level of linear correlation at 3 and 8 kHz is smaller than at frequencies below 3 kHz. This suggests that wind contribution to γ ANL is partly masked by distant biotic contributions (chorus).

The wind speed dependence model for coastal areas presented here takes into account masking properties of benthic sounds. The model includes a constant floor component and a log-affine law of power spectral density. A key parameter of the model is the transition wind speed which indicates the minimum wind speed required for the wind-induced sound contribution to be above the benthic biophony noise floor. At 400 Hz, the transition wind speed is small (i.e., 3 kn) for both γ RL and γ ANL and the probability that the acoustic wind contribution is masked by benthic sounds is very low (only

TABLE II. Distribution of overall ocean noise level (γ_{RL}) and background ambient noise level (γ_{ANL}) at 400 Hz, 3 kHz, and 8 kHz.

Level [dB re 1 μPa^2]	Mean	Std	1%	5%	10%	25%	50%	75%	90%	95%	99%
γ_{RL}, 400 Hz	65.17	7.39	49.1	52.44	55.29	60.83	65.27	69.19	74.13	78.3	85.02
γ_{ANL}, 400 Hz	59.7	6.5	46.26	48.6	50.94	54.87	59.98	64.19	68.14	70.16	73.84
γ_{RL}, 3 kHz	68.28	2.03	64.05	65.25	65.87	66.92	68.18	69.5	70.76	71.56	73.32
γ_{ANL}, 3 kHz	61.07	2.6	54.99	56.81	57.81	59.43	61.11	62.68	64.11	64.99	67.29
γ_{RL}, 8 kHz	59.59	2.13	54.98	56.27	56.98	58.19	59.53	60.91	62.19	63.01	64.9
γ_{ANL}, 8 kHz	53.31	2.27	48.71	49.75	50.4	51.75	53.33	54.76	55.94	56.67	58.86

TABLE III. Pearson's correlation coefficient between noise levels (γ_{RL} and γ_{ANL} at 400 Hz, 3 kHz, and 8 kHz) and the binary logarithm of wind speed during the period from June 26, 2011 to July 26, 2011 and during the full period of the experiment, from June 20, 2011 to November 13, 2011.

	Correlation coefficient June 26 to July 26 2011	Correlation coefficient June 20 to November 13 2011
$\gamma_{RL\ 400Hz}$, $\log_2(W)$	0.70	0.52
$\gamma_{ANL\ 400Hz}$, $\log_2(W)$	0.81	0.68
$\gamma_{RL\ 3kHz}$, $\log_2(W)$	0.09	0.16
$\gamma_{ANL\ 3kHz}$, $\log_2(W)$	0.40	0.46
$\gamma_{RL\ 8kHz}$, $\log_2(W)$	0.07	0.06
$\gamma_{ANL\ 8kHz}$, $\log_2(W)$	0.35	0.31

3% of measured wind speeds are smaller than 3 kn (cf. Table I). The transition wind speed for γ ANL increases at 3 kHz (9.9 kn) and 8 kHz (11.8 kn) suggesting an increasing masking effect of the benthic chorus (40% of measured wind speeds are higher than 9.9 kn).

Another way to evaluate the magnitude of wind dependence of the spectral density is to investigate the proportion of spectral density variance explained by the model (cf. values of R^2 in Table IV). The model explains only a small proportion of variance for the γ RL at 3 kHz (4%) and 8 kHz (1%), and the dependence is not significant. The proportion of the variance explained by the wind dependence is always higher for the γ ANL than for the γ RL (by a factor of 2 at 400 Hz, a factor of 5 at 3 kHz and a factor of 10 at 8 kHz). Although the wind dependence of the γ ANL is always significant, the proportion of variance explained by the wind speed decreases with increasing frequency (47% at 400 Hz, 23% at 3 kHz, and 11% at 8 kHz). The remaining variability can be likely attributed to the variable diurnal contribution of benthic chorus and changes in transmission loss caused by tides (±3 m tidal range in a 10 m water depth) (see Fig. 8).

Finally, for wind speeds greater than the transition wind speed, the logarithmic model for the wind dependence of spectral levels is appropriate as indicated by the similar slopes of γ RL at 400 Hz and γ ANL at 3 kHz and 8 kHz (between 26 and 28 dB per decade).

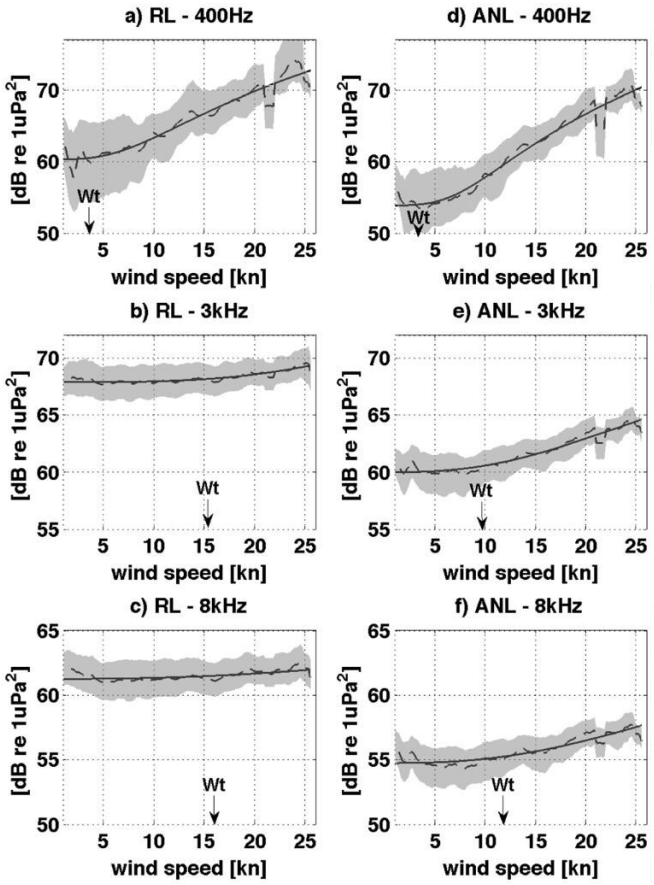

FIG. 7. (a–c) Comparison of measured and modeled overall ocean noise level (γ_{RL}) at 400 Hz, 3 kHz, and 8 kHz for varying wind speeds during the 5 month dataset. The dashed line corresponds to the 50th percentile of the measured ocean noise level at each given frequency. The shaded area corresponds to levels between the 25th and the 75th percentiles. The solid line corresponds to the modeled overall ocean noise level, computed using all the measured received levels at each given frequency. The transition wind speed W_c is also displayed. (d-f) Same as above but for background ambient noise level (γ_{ANL}).

B. Comparison of ambient noise wind dependence with earlier studies

Necessary information for a comparison with earlier studies is summarized in Table V and includes site water depth, biological sources, model used to study wind dependence, and relevant results.

The variability among studies of noise levels in absence of wind indicates that shallow water measurements are highly site-dependent, due to differences in water depth, bottom composition and propagation conditions, as discussed by Ingenito and Wolf (1989). For instance, Ramji *et al.* (2008) reported that the wind-generated noise level measured in the Bay of Bengal during the summer was up to 8 dB smaller than during the winter and monsoon season. They attributed this difference to the sound speed profile variation.

To our knowledge, no previous wind-dependent noise analysis has mentioned the contribution of benthic sounds. McDonald *et al.* (2008), Ramji *et al.* (2008), and Nystuen *et al.* (2010) excluded periods contaminated with non-surface wind-generated noise sources (shipping, rain, marine mammals) from their analysis. The particularity of the Iroise Sea study site and likely of many other rocky or coral reef environments, is the presence of a biological chorus even when transient contributions have been removed. The ambient noise level in absence of wind is 54 dB re 1 mPa^2/Hz at 400 Hz and 60 re 1 mPa^2/Hz at 3 kHz, which falls within the range of values reported by previous studies. The 6 dB difference is attributed to the biological chorus present at frequencies above 1 kHz.

Except for Poikonen and Madekivi (2010), all previous studies reported a linear relationship at all frequencies between the noise level and the logarithm of the wind speed. This relationship accounts for wind speeds above 4 kn, which corresponds to the threshold wind speed of a breaking wave. Poikonen and Madekivi (2010) used a three-region model to describe wind speed dependence. The first region was a constant noise region below the critical wind speed threshold (no breaking waves). The transition region was determined by the wind speed corresponding to the onset of

TABLE IV. Model curve parameters (Q_f, Q_1, and k) used to produce Fig. 7. These parameters result from the wind-based fit between measured and modeled overall ocean noise levels (γ_{RL}) and background ambient noise levels (γ_{ANL}) at 400 Hz, 3 kHz, and 8 kHz. The transition wind speed W_t is derived using Eq. (4). The resulting explained variance (R^2) and explained variance for winds above W_t ($R^2_{W>Wt}$) are also displayed. F-statistic values (F-stat) larger than the critical value for $p = 0.05$ are in italic.

	Q_f (std)	Q_1 (std)	k (std)	W_t (std)	R^2	$R^2_{W>Wc}$	F-stat
γ_{RL}, 400 Hz	55.9 (0.6)	31.5 (1.2)	28.5 (1.9)	3.3 (0.2)	0.27	0.32	*680*
γ_{ANL}, 400 Hz	53.8 (0.4)	20.2 (0.9)	35.3 (1.3)	2.9 (0.4)	0.47	0.54	*773*
γ_{RL}, 3 kHz	67.9 (0.1)	14.5 (10.9)	34.1 (7.9)	15.5 (3.5)	0.04	0.09	210
γ_{ANL}, 3 kHz	59.8 (0.2)	25.5 (1.7)	26.9 (1.5)	9.9 (0.3)	0.23	0.28	*457*
γ_{RL}, 8 kHz	60.4 (0.9)	−18.1 (31.2)	40.6 (22.6)	16.1 (4.1)	0.01	0.02	154
γ_{ANL}, 8 kHz	53.6 (1.0)	16.3 (2.5)	26.0 (2.3)	11.8 (0.9)	0.11	0.20	*344*

breaking waves. Above this transition wind speed, the noise level raised with increasing wind speed at a rate determined by the wind speed dependence factor k. The third region was characterized by wind speed saturation in terms of fully developed sea state conditions at which the noise level starts to saturate. The wind speed dependence of background ambient noise levels observed in this study is similar to the one described by Poikonen and Madekivi (2010), who used the γ RL acoustic descriptor (spectrum levels of overall ocean noise). Here, a saturation wind speed is not observed, although 10% of the wind speed values are higher than 20 kn (Table I). Unlike Poikonen and Madekivi (2010), the wind speed threshold is highly dependent on the frequency and its relation to the masking potential of the biological chorus above 1 kHz. The variance explained by the wind decreases as frequency increases. This is similar to results reported by Ramji *et al.* (2008), who indicated a strong correlation coefficient between the noise spectrum level and wind speed at 500 Hz ($r = 0.93$) that decreased with increasing frequency, with a minimum value of 0.06 at 5 kHz during the winter. Given the shallow water environment in the study by Ramji *et al.* (2008) (Bay of Bengal), a biological masking by benthic species (such as snapping shrimps) at frequencies above 1 kHz can be expected and likely explains the similarities with our results.

The frequency range of the wind-dependence of ambient noise level reported here was [0.1–14 kHz]. Nystuen *et al.* (2010) reported a wind dependence up to 30 kHz. This difference can be attributed to the very shallow depth of the study site of the here presented work (10 m at high tide). Table V also permits to compare the wind speed dependence slope, here reported in dB per decade. In this study, the wind speed dependence factor k varies between 26.6 and 35.9 dB/decade depending on the frequency. These values are in good agreement with those reported by previous studies, thus showing that the γ ANL descriptor used here allows recovering wind speed dependence in a biologically rich coastal area.

C. Effects of tidal currents, sound speed profile, and bottom type on noise properties

The potential effects of several environmental factors on noise levels were examined to assess how they influence the wind dependence of spectral levels.

1. Tidal currents

The coastal study site is associated with strong tidal currents up to 1 m/s [average value of 0.40 (+/−0.17) m/s] [Previmer database, MARS2D model; Previmer (2016)] which can generate cable-strumming and broadband noise. As mentioned previously in Sec. II B, the deployment technique did not require a mooring line and therefore strongly limited strumming noise. Cable strumming was only observed between July 6 and July 9, a period associated with high wind events. It was present in the [10–12] kHz frequency range. Since the analysis was made in narrow frequency bands around 400 Hz, 3 kHz, and 8 kHz, we assumed that estimated noise levels were not impacted by cable strumming. Additionally the Kinda *et al.* (2013) algorithm removes cable- strumming noises when computing the γ ANL descriptor. The relationship between spectral levels γ ANL at 400 Hz, 3 kHz, and 8 kHz and current speed were examined (obtained from the Previmer dataset) for the whole 5-month dataset. No linear or second-order relationship were found, we therefore assumed that it did not influence the

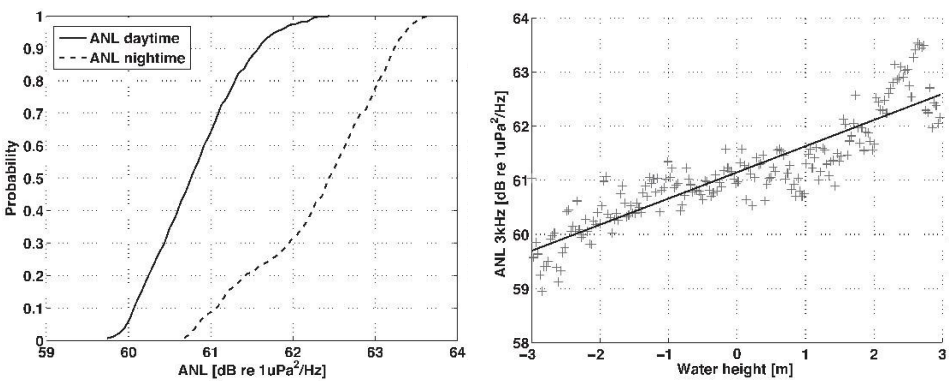

FIG. 8. (left) Cumulative distributive function (CDF) of background ambient noise level (γ_{RL}) at 3 kHz during day time and during night time, for the period from June 26 to July 26, 2011 showing a ~2 dB difference between nighttime and daytime γ_{ANL}. (right) γ_{RL} at 3 kHz as a function of water height (cross), for the period from June 26 to July 26, 2011 showing a ~3 dB variation of γ_{ANL} with water height changes due to tides. The straight line shows the linear regression.

TABLE V. Main characteristics of previous shallow water studies on wind dependence of ambient noise.

	Depth	Biological sources	Analysis/Model	Wind speed dependence frequency range	Noise level absence of wind (dB re $1\mu Pa^2/Hz$)	Wind speed threshold	Slope (initial descriptor)	Slope (dB/decade)
Ingenito and Wolf (1989)	<50 m	Not mentioned	Noise spectrum level for various wind speed conditions	0.1–1.5 kHz (entire study band)	52 dB at 1 kHz	4 kn	[1.4 2.1] dB/kn	[18–32]
Ma *et al.* (2005)	20–98 m	Not mentioned	Vagle *et al.* (1990) empirical algorithm	1–50 kHz	53 dB at 1 kHz	4 kn	[20] dB/decade	[20]
McDonald *et al.* (2008)	110 m	Periods with blue and fin whale calls not included in the analysis	200 sec spectral averages	10–220 Hz (entire study band)	55 dB at 10 Hz	Not mentioned	[1–6] dB/octave	[3–18]
Ramji *et al.* (2008)	5–15 m	Periods when dolphins present not included in the analysis	Noise level linear to the logarithm of the wind speed	0.5–6 kHz (entire study band)	70 dB at 1 kHz	4 kn	[3–19] dB/decade	[3–19]
Nystuen *et al.* (2010)	70 m	Non-stationary signal between 3 and 15 kHz was rejected as noise	Vagle *et al.* (1990) empirical algorithm	0.1–30 kHz (entire study band)	44 dB at 1 kHz	6 kn	[20] dB/decade	[20]
Poikonen and Madekivi (2010)	20 m	Not mentioned	Four-parameter logarithmic model	60 Hz–10 kHz	43 dB at 1 kHz	5 kn	[21–49] dB/decade	[21–49]

wind dependence of spectral levels reported in the preceding sections.

2. Sound speed profile and seasonality

The shallow study site is associated with an isovelocity sound profile. An Aanderaa sensor measured temperature continuously at 3 m depth between July 1 and July 21. A simulation of the oceanic distribution of temperature in the Iroise Sea was made during the same period [Stéphan (2016); SHOM, code MARS3D]. Validation of the simulation model was obtained by comparing the measured and modeled water temperature (temperature difference lower than 1 °C, same temporal variability). The model reveals a well-mixed water column during the whole measuring period (180 days), except for two 3-day span periods (corresponding to the Ushant front passing above our sensor at the end of spring and in the beginning of autumn). When examining noise seasonality no significant difference in noise levels between months was found. The number of high wind speed events during each month is the factor influencing the most the average noise level. The high wind speed events were well distributed during the 5-month measuring period [mean wind speed (± standard deviation) during each month: June, 12.5 kn (±3.7); July, 11.1 kn (±5.2); August, 9.6 kn (±4.1); September, 12.79 kn (±5.7); October, 12.83 kn (±5.8); and November, 13.5 kn (±5.5)]. Therefore, variations in propagation conditions due to seasonal variations do not affect our acoustic dataset.

3. Bottom type

Bottom properties of the deployment location correspond to infralittoral coarse sediments. Sediment type drives two major characteristics of the soundscape: (i) the propagation of sound sources (through bubbles at the surface and benthic fauna at the bottom) and (ii) the presence of biological sound sources (sediment type determine the presence of benthic communities). Consequences of sediment type on sound propagation (soft sediments enable the propagation of nearby sound sources, do not favor the propagation of distant wind-induced noise, and therefore enable the masking of wind noise by biological sounds) are less important than the consequences of the presence or absence of benthic sound sources (also conditioned by sediment type). Sound producing benthic species mainly inhabit hard substrate (gravels, rocks), can be found on mixed habitats (e.g., maërl), but are rarely found on soft substrate (sand, silt) (Johnson *et al.*, 1947; Radford *et al.*, 2010; McWilliam and Hawkins, 2013; Lillis *et al.*, 2014). These four publications show that the biological sound level for a hard sediment habitat (hosting a rich sound producing benthic community) is 15 to 20 dB higher than for a soft sediment habitat (hosting a poor sound producing benthic community). An ANL sound reduction of 20 dB at a 3 kHz frequency will be applied on the Q_f model parameter (constant floor corresponding to the biological and the anthropogenic contributions) and induces a reduction of the transition wind speed W_t by a factor of 5 (2 kn instead of 9.9 kn). Considering the distribution of wind speeds in our study area, $W_t = 9.9$ kn corresponds to a masking of wind

noise by biological sound sources 50% of the time, compared to only 2% of the time for $W_t = 2$ kn.

VI. CONCLUSION

In this study, we demonstrated that the wind dependence of spectral levels is primarily a question of masking when working in a biologically rich coastal soundscape. When dealing with overall ocean noise [γ RL(f)] the wind dependence of spectral level was not significant for frequencies associated with zoobenthic transient sounds. We used an algorithm to automatically filter out this loud biophonic contribution and estimate the background ambient noise spectrum level [γ ANL(f)]. The wind dependence of γ ANL was significant at all frequencies. The richness of the soundscape was taken into account when proposing a logarithmic model for γ ANL. Thanks to this model, we demonstrated that wind dependence holds on once wind speed was high enough to produce sounds exceeding the zoobenthic chorus. For these high wind speeds, a logarithmic affine law was adequate, and its estimated parameters were compatible with previous shallow water studies. Wind speed explained as much as 47% of the background ambient noise level variance. Natural variation of the biophony and change of water depth is responsible for some of the remaining variance.

ACKNOWLEDGMENTS

This work was supported by ANR-12-ASTR-0021-03 MER CALME. The authors thank Jérôme Mars for his valuable comments on the manuscript.

Barclay, D. R., and Buckingham, M. J. (**2013**). "Depth dependence of wind-driven, broadband ambient noise in the Philippine Sea," J. Acoust. Soc. Am. **133**(1), 62–71.

Di Iorio, L., Gervaise, C., Jaud, V., Robson, A., and Chauvaud, L. (**2012**). "Hydrophone detects cracking sounds: Non-intrusive monitoring of bivalve activity," J. Exp. Mar. Biol. Ecol. **432**, 9–16.

Evans, D. L., Watts, D. R., Halpern, D., and Bourassa, S. (**1984**). "Oceanic winds measured from the seafloor," J. Geophys. Res. **89**, 3457–3461, doi:10.1029/JC089iC03p03457.

Falkowski, P. G., Barber, R. T., and Smetacek, V. (**1998**). "Biogeochemical controls and feedbacks on ocean primary production," Science **281**(5374), 200–206.

Gaul, R. D., Knobles, D. P., Shooter, J. A., and Wittenborn, A. F. (**2007**). "Ambient noise analysis of deep-ocean measurements in the Northeast Pacific," IEEE J. Oceanic Eng. **32**(2), 497–512.

Gervaise, C., Simard, Y., Roy, N., Kinda, B., and Ménard, N. (**2012**). "Shipping noise in whale habitat: Characteristics, sources, budget, and impact on belugas in Saguenay-St. Lawrence Marine Park hub," J. Acoust. Soc. Am. **132**(1), 76–89.

Hazen, M. G., and Desharnais, F. (**1997**). "The Eastern Canada shallow water ambient noise experiment," Proc. IEEE Oceans **1**, 471–476.

Hildebrand, J. A. (**2009**). "Anthropogenic and natural sources of ambient noise in the ocean," Mar. Ecol. Prog. Ser. **395**(5), 5–20.

Ingenito, F., and Wolf, S. N. (**1989**). "Site dependence of wind-dominated ambient noise in shallow water," J. Acoust. Soc. Am. **85**(1), 141–145.

Johnson, M. W., Everest, F. A., and Young, R. W. (**1947**). "The role of snapping shrimp (Crangon and Synalpheus) in the production of underwater noise in the sea," Biol. Bull. **93**, 122–138.

Kay, S. M. (**1998**). "Fundamentals of statistical signal processing, Vol. II: Detection Theory," in *Signal Processing* (Prentice Hall, Upper Saddle River, NJ).

Kinda, G. B., Simard, Y., Gervaise, C., Mars, J. I., and Fortier, L. (**2013**). "Under-ice ambient noise in Eastern Beaufort Sea, Canadian Arctic, and its relation to environmental forcing," J. Acoust. Soc. Am. **134**(1), 77–87.

Knudsen, V. O., Alford, R. S., and Emling, J. W. (**1948**). "Underwater ambient noise," J. Mar. Res. **7**, 410–429.

Lagarias, J. C., Reeds, J. A., Wright, M. H., and Wright, P. E. (**1998**). "Convergence properties of the Nelder Mead simplex method in low dimensions," SIAM J. Optim. **9**(1), 112–147.

Lee, T. N., Rooth, C., Williams, E., McGowan, M., Szmant, A. F., and Clarke, M. E. (**1992**). "Influence of Florida Current, gyres and wind-driven circulation on transport of larvae and recruitment in the Florida Keys coral reefs," Cont. Shelf Res. **12**(7-8), 971–1002.

Lemon, D., Farmer, D. M., and Watts, D. R. (**1984**). "Acoustic measurements of wind speed and precipitation over a continental shelf," J. Geophys. Res. **89**, 3462–3472, doi:10.1029/JC089iC03p03462.

Lillis, A., Eggleston, D. B., and Bohnenstiehl, D. (**2014**). "Estuarine soundscapes: Distinct acoustic characteristics of oyster reefs compared to soft-bottom habitats," Inter-Res. Mar. Ecol. Prog. Ser. **505**, 1–17.

Ma, B. B., Nystuen, J. A., and Lien, R. C. (**2005**). "Prediction of underwater sound levels from rain and wind," J. Acoust. Soc. Am. **117**(6), 3555–3565.

Marshall, S. W. (**2005**). "Depth dependence of ambient noise," IEEE J. Ocean Eng. **30**, 275–281.

McDonald, M. A., Hildebrand, J. A., Wiggins, S. M., and Ross, D. (**2008**). "A 50 year comparison of ambient ocean noise near San Clemente Island: A bathymetrically complex coastal region off Southern California," J. Acoust. Soc. Am. **124**(4), 1985–1992.

McWilliam, J. N., and Hawkins, A. D. (**2013**). "A comparison of inshore marine soundscapes," J. Exp. Mar. Biol. Ecol. **446**, 166–176.

Medwin, H., and Beaky, M. (**1989**). "Bubble sources of the Knudsen sea noise spectra," J. Acoust. Soc. Am. **86**(3), 1124–1130.

Mellinger, D., Stafford, K., Moore, S., Dziak, R., and Matsumoto, H. (**2007**). "An overview of fixed passive acoustic observation methods for cetaceans," Oceanography **20**(4), 36–45.

Morris, G. B. (**1978**). "Depth dependence of ambient noise in the northeastern Pacific Ocean," J. Acoust. Soc. Am. **64**, 581–590.

National Research Council (**2003**). *Ocean Noise and Marine Mammals* (National Academies, Washington, DC).

Nystuen, J. A., McGlothin, C. C., and Cook, M. S. (**1993**). "The underwater sound generated by heavy rainfall," J. Acoust. Soc. Am. **93**(6), 3169–3177.

Nystuen, J. A., Moore, S. E., and Stabeno, P. J. (**2010**). "A sound budget for the southeastern Bering Sea: Measuring wind, rainfall, shipping, and other sources of underwater sound," J. Acoust. Soc. Am. **128**(1), 58–65.

Perrone, A. J. (**1970**). "Ambient-noise-spectrum levels as a function of water depth," J. Acoust. Soc. Am. **48**(1), 362–370.

Piggott, C. L. (**1964**). "Ambient sea noise at low frequencies in shallow water of the Scotian Shelf," J. Acoust. Soc. Am. **36**(11), 2152–2163.

Pijanowski, B. C., Villanueva-Rivera, L. J., Dumyahn, S. L., Farina, A., Krause, B. L., Napoletano, B. M., Gage, S. H., and Pieretti, N. (**2011**). "Soundscape ecology: The science of sound in the landscape," BioScience **61**(3), 203–216.

Poikonen, A., and Madekivi, S. (**2010**). "Wind-generated ambient noise in a shallow brackish water environment in the archipelago of the Gulf of Finland," J. Acoust. Soc. Am. **127**(6), 3385–3393.

Post, E., Forchhammer, M. C., Bret-Harte, M. S., Callaghan, T. V., Christensen, T. R., Elberling, B., Fox, A. D., Gilg, O., Hik, D. S., Høye, T. T., Ims, R. A., Jeppesen, E., Klein, D. R.,Madsen J., McGuire, A. D., Rysgaard, S., Schindler, D. E., Stirling, I., Tamstorf, M. P., Tyler, N. J., van der Wal, R., Welker, J., Wookey, P. A., Schmidt, N. M., and Aastrup, P. (**2009**). "Ecological dynamics across the Arctic associated with recent climate change," Science **325**(5946), 1355–1358.

Previmer (**2016**). "Previmer," http://www.previmer.org (Last viewed February 6, **2016**).

Prosperetti, A., and Oguz, H. (**1993**). "The impact of drops on liquid surfaces and the underwater noise of rain," Ann. Rev. Fluid Mech. **25**(1), 577–602.

Radford, C., Jeffs, A., Tindle, C., and Montgomery, J. C. (**2008**). "Resonating sea urchin skeletons create coastal choruses," Mar. Ecol. Prog. Ser. **362**, 37–43.

Radford, C., Stanley, J., Tindle, C., Montgomery, J., and Jeffs, A. (**2010**). "Localised coastal habitats have distinct underwater sound signatures," Mar. Ecol. Prog. Ser. **401**, 21–29.

Raffin, C. (**2004**). "Biological and ecological bases for the conservation of the marine environment in the Iroise Sea," Ph.D. thesis, University of Western Brittany, Brest, France.

Ramji, S., Latha, G., Rajendran, V., and Ramakrishnan, S. (**2008**). "Wind dependence of ambient noise in shallow water of Bay of Bengal," Appl. Acoust. **69**(12), 1294–1298.

Riser, S. C., Nystuen, J., and Rogers, A. (**2008**). "Monsoon effects in the Bay of Bengal inferred from profiling float-based measurements of wind speed and rainfall," Limnol. Oceanogr. **53**(5), 2080–2093.

Rountree, R., Gilmore, R., Goudey, C., Hawkins, A., Luczkovich, J., and Mann, D. (**2006**). "Listening to Fish," Fisheries **31**(9), 433–446.

Schofield, O., Ducklow, H. W., Martinson, D. G., Meredith, M. P., Moline, M. A., and Fraser, W. R. (**2010**). "How do polar marine ecosystems respond to rapid climate change?," Science **328**(5985), 1520–1523.

Sousa-Lima, R. S., Norris, T. F., Oswald, J. N., and Fernandes, D. P. (**2013**). "A review and inventory of fixed autonomous recorders for passive acoustic monitoring of marine mammals," Aquat. Mamm. **39**(1), 23–53.

Stéphan, Y. (**2016**). (personal communication).

Talidec, C., Boncoeur, J., Alban, F., Curtil, O., Le Floc'h, P., Le Gallic, B., Pennanguer, S., Berthou, P., Fifas, S., and Latrouite, D. (**2002**). "Report 2001: Scenarios for the development of the fishing activities on the Brittany coast (Ifremer, Brest)," pp. 29–37.

Urick, R. J. (**1984**). "Ambient noise in the sea," Undersea Warfare Technology Office, Naval Sea System Command, Department of the Navy, Washington, DC.

Vagle, S., Large, W. G., and Farmer, D. M. (**1990**). "An evaluation of the WOTAN technique of inferring oceanic winds from underwater ambient sound," J. Atmos. Oceanic Technol. **7**(4), 576–595.

Vakkayil, R., Graber, H. C., and Large, W. G. (**1996**). "Oceanic winds estimated from underwater ambient noise observations in SWADE," Proc. IEEE Oceans **41**, 45–51.

Vandemeulebrouck, J., Sabroux, J., Halbwachs, M., Poussielgue, N., Grangeon, J., and Tabbagh, J. (**2000**). "Hydroacoustic noise precursors of the 1990 eruption of Kelut Volcano, Indonesia," J. Volcanol. Geotherm. Res. **97**(1–4), 443–456.

Walsh, J. J., Whitledge, T. E., Barvenik, F. W., Wirick, C. D., Howe, S. O., Esaias, W. E., and Scott, J. T. (**1978**). "Wind events and food chain dynamics within the New York Bight," Limnol. Oceanogr. **23**(4), 659–683.

Watanabe, M., Sekine, M., Mamada, E., Ubika, M., and Imai, T. (**2002**). "Monitoring of shallow sea environment by using snapping shrimps," Water Sci. Technol. **46**(11), 419–424.

Wenz, G. M. (**1962**). "Acoustic ambient noise in the ocean: Spectra and sources," J. Acoust. Soc. Am. **34**, 1936–1957.

Weston, D. E., and Ching, P. A. (**1989**). "Wind effects in shallow-water acoustic transmission," J. Acoust. Soc. Am. **86**(4), 1530–1545.

Wille, P. C., and Geyer, D. (**1984**). "Measurements on the origin of the wind-dependent ambient noise variability in shallow water," J. Acoust. Soc. Am. **75**(1), 173–185.

Zakarauskas, P., Chapman, D. M., and Staal, P. R. (**1990**). "Underwater acoustic ambient noise levels on the eastern Canadian continental shelf," J. Acoust. Soc. Am. **87**(5), 2064–2071.

Zedel, L., Gordon, L., and Osterhus, S. (**1999**). "Ocean ambient sound instrument system: Acoustic estimation of wind speed and direction from a subsurface package," J. Atmos. Oceanic Technol. **16**(8), 1118–1126.